International Journal on Advanced Science Engineering Information Technology

Vol.12 (2022) No. 2
ISSN: 2088-5334

# Determination of the Appropriate Number of Photovoltaic Panels for Microgeneration and Self-supply of Final Consumers by Energy Production Estimation via Fuzzy Logic

Cristhian Chávez [a], Juan David Ramírez [a,*], María Fernanda Trujillo L. [b], Patricia Otero [a], Sebastián Taco-Vásquez [c], Víctor Tibanlombo [a]

[a] *Departamento de Energía Eléctrica, Escuela Politécnica Nacional, Ladrón de Guevara E11 253 Quito, Ecuador*
[b] *Departamento de Ingeniería Mecánica, Escuela Politécnica Nacional, Ladrón de Guevara E11 253 Quito, Ecuador*
[c] *Departamento de Ingeniería Química, Escuela Politécnica Nacional, Ladrón de Guevara E11 253 Quito, Ecuador*
*Corresponding author: *juan.ramirezd@epn.edu.ec*

***Abstract*— A method is presented to determine the appropriate number of photovoltaic panels that should be installed in an end-user photovoltaic installation to guarantee the supply of energy to the load during the hours of solar radiation, according to factors such as the installation area and global solar radiation. Solar radiation is predicted by approximating the daily distribution of global irradiance through a Gaussian function, which is subsequently corrected using a heuristic approach. Meteorological parameters are used as input data such as the daily solar insolation and the maximum global irradiance for each day; this last parameter is obtained through an expert system based on fuzzy logic that was programmed and trained with the data of ambient temperature and relative humidity that were obtained in the processing stage. Output from this expert system is the predicted values of maximum radiation obtained for each day for a selectable time interval. With the predicted solar radiation, the generation of electrical energy from the photovoltaic panels is calculated. The load is randomly modeled from a pattern of the energy demand of the building to be powered by the photovoltaic system. The number of photovoltaic panels needed is found with the information acquired in the previous stages and the information of the energy demand of the load and the installation area. The results are the number of solar panels that would be needed at all hours of the day from which the radiation prediction was made.**

***Keywords*— Fuzzy logic; prediction of solar radiation; photovoltaic systems; capital recovery time; energy production estimation.**

*Manuscript received 21 Apr. 2021; revised 1 Sep. 2021; accepted 13 Nov. 2021. Date of publication 30 Apr. 2022.*


## I. INTRODUCTION

Ecuador has implemented regulations to increase the use of solar power recently. For instance, the country created the Electricity Regulation and Control Agency (ARCONEL), an organization that regulates and controls the technical, economic, and operational aspects of the electric public service power activities. In October 2018, ARCONEL issued regulation 003/18 that allows the installation of photovoltaic systems for self-supply, allowing end consumers can install these systems in their homes and obtain both photovoltaic electrical energy and network energy [1].

ARCONEL regulation 003/18 item 12 states that a photovoltaic system can generate energy surpluses when commercial treatment of energy produced from low-capacity photovoltaic systems and is needed to perform an analysis of the different cases, which could occur at the same time. The regulation also states that when there are surpluses of energy from the photovoltaic system, these can be injected into the distribution company's low or medium voltage network, and the payment of energy is made from a monthly net energy balance mechanism. In this case, the distribution company oversees making the economic balance of the energy monthly, considering the records of injected or consumed energy flows that can be measured from bidirectional measurement equipment.

Electrical companies calculate the monthly net balance of energy received and consumed by the customer using the photovoltaic microsystem within the first ten days of the month after the operation of the photovoltaic microsystem. When the result of this net monthly energy balance is negative, the electrical company evaluates energy consumption according to the corresponding tariff found in the ARCONEL tariff schedule. As well, it also emphasizes that a negative remainder is not subject to subsidies.

When the positive net monthly balance result is positive, the positive remainder of energy favors the consumer and is considered an energy credit that will be passed on to the next month and so on successively until it reaches a maximum period called reset. This energy credit reset period is two years, from the date the operation of the photovoltaic microsystem was authorized until there is a cause for the disconnection of the photovoltaic microsystem or the term of operation that is equal to 20 years is fulfilled.

A profitability study is needed because it is enough to know the number of panels needed and whether the calculated number of photovoltaic panels is not an excessive expense at the time of their acquisition in the market. The cost of photovoltaic generation depends on the equipment investment, operation, maintenance cost, the energy delivered by the panels, and the capacity factor [2]–[5]. The installation place, including its dimensions, is important because the load, lifetime of the photovoltaic panel, and the available space of the building could not be enough for the number of panels calculated [6].

This article studies a method to find the number of suitable photovoltaic panels for any type of photovoltaic installation for end-users, using a practical example, for which algorithm programming is developed in MATLAB® software.

This document is based on the Zervas et al. strategy, which consists of two parts: a) to use Gaussian type function to be able to predict the daily distribution of total solar irradiance, and b) calculate the value of the amplitude of the Gaussian function using neural networks or some type of regressor [7].

Artificial neural network training algorithms are quick and robust [8]; however, they have some drawbacks [9], [10], such as the topology scheme of a conventional neural network is calculated when the centers of the hidden nodes are selected, and it would require performing several executions passes for each of the training examples, increasing the computational effort. This occurs when there is a high amount of data in a database. On the other hand, artificial neural network training algorithms depend on a random selection at the beginning of the centers of the nodes having different sets of centers for each simulation carried out in the same network structure; however, using fuzzy logic is possible to overcome these disadvantage [11]–[15].

Fuzzy logic is advantageous over conventional neural networks because fuzzy logic is based on the partition for an input space. Both the structure and the centers of the nodes are chosen in a single step when passing a single one for the training examples [16]–[18]; As well, there will be the same set of centers for a fuzzy partition given its input space, which prevents many simulations from being carried out because this time there are no random selections of centers within the algorithm [11], [16], [17].

The radiation, relative humidity, and ambient temperature data are obtained from the Environment Secretariat of the Metropolitan District of Quito website, which is in EXCEL format. Later, these data will be extracted through a script programmed in MATLAB®, in a data preprocessing stage. It is required to select the most important data to develop the following stages of this project. For this preprocessing stage, the data is obtained on the one hand the highest values during each day for the last two years. On the other hand, for global solar radiation, relative humidity, and ambient temperature, the global solar radiation data is collected for each day for the hours of sunlight during the last two years.

The code was written to find a function to approximate the daily distribution of global solar irradiance in the Metropolitan District of Quito, especially in places near the Belisario Quevedo meteorological station, which is where all the data are obtained from global solar irradiance.

A correction is made in that function so that the results are as close as possible to reality. This last function requires a fundamental parameter such as the maximum global solar irradiance or amplitude based on the processed data. For this study, this data prediction is based on the useful life of the photovoltaic panel that is chosen as an example. To execute this prediction, an algorithm based on Fuzzy Logic is carried out. The inputs such as radiation, ambient temperature, relative humidity, and output yields the predicted results of global solar radiation are 730 values; the algorithm is trained with all the data obtained in the preprocessing stage.

Then the appropriate number of photovoltaic panels is found by using a mathematical relationship describing the behavior of a photovoltaic panel that includes the global solar distribution and the load demand used as an example, in addition to other related parameters with the photovoltaic panel.

With the appropriate number of photovoltaic panels found, the electrical power in the time delivered by the system is determined by the connected demand, and it is compared if the results will be correct by using SIMULINK®, which two curves are obtained that represent the power in the time that the photovoltaic system delivers the load and the demand respectively. Therefore, there is a difference between areas of both curves whose physical meaning represents the remaining or surplus energy the photovoltaic system responds.

In this study, the appropriate selection of the number of photovoltaic panels is proposed on the basis that the energy delivered by the installation during each day can cover most of the energy needed by the load so that the net consumption of the electrical network will be as low as possible so that energy savings make it possible to amortize the investment of the photovoltaic installation. Considering the maximum use of the available areas and avoiding the oversizing since the excess energy produced is not invoiced.

## II. Materials and Method

### A. Data Preprocessing

The Environment of the City of Quito Secretary 's website of the [19] has historical data from the Metropolitan Network for Atmospheric Monitoring (REMMAQ) that are reliable data about the concentration of atmospheric pollutants within the city of Quito.

REMMAQ has 9 monitoring stations that are continuously analyzing air quality in the city. From these nine stations, six have remote automatic monitoring stations which measure some parameters, such as wind speed and direction, solar radiation, humidity, precipitation, and pressure. The meteorological stations are installed on the roof of the monitoring stations. In addition, there is a control center that receives, stores and processes the information registered by the monitoring stations.

The data found on the Quito Environment Secretariat website are free of charge to use, and have kept historical data from the mid-2000s, and are updated every hour since 2000 to the current time. It must be emphasized that there were no data for certain hours on certain days of several years because of the failure of the measurement process at that time.

The data collected from this database were ambient temperature, relative humidity, and radiation. All of them are sorted so that the peak value of each variable is obtained for each day from January 1st, 2018, and only those belonging to the Belisario Quevedo meteorological station.

The data extracted from the EXCEL file is filtered with a script. Data are ordered and after its extraction through the script called "data" and then are saved in another script called "extracted data". The extracted data had a visual inspection and a final inspection to verify that there were no days without assigned values. After the inspection, there were few days with no values and were assigned the corresponding value of a day before or a day after, according to a realistic allocation. Finally, in the "extracted data" script, three vectors are saved with the required parameters' data: radiation, ambient temperature, and relative humidity. Both relative humidity and ambient temperature have a total of 730 elements equivalent to two years. However, the radiation vector has 790 data representing two years plus the months of January and February 2020.

### *B. The Division of Fuzzy Subspaces*

Upper and lower limits of the entry space are determined for humidity, temperature, and radiation. The minimum of the values extracted in the data preprocessing stage minus 10% of the range's data values is used as a reference for the lower limit. In addition, the maximum value of the data plus 10% of the range of values is used for the maximum limit. Thus, the maximum and minimum values of the variables are:

Minimum temperature: 11.19 °C
Maximum temperature: 24.03 °C
Minimum humidity: 39.695 %
Maximum humidity: 100 %
Minimum radiation: 164.18 W/m2
Maximum radiation: 1219.2 W/m2

For the subdivision of fuzzy subspaces, the part of the input space for each variable is equal to 2 * N + 1. In this case, there is a homogeneous division for each variable equal to N = 9, resulting in 19 subspaces.

As a strategy to determine the degree of membership for each variable, each variable is taken one by one, then the mathematical process corresponding to (1.a) and (1.b) is carried out [6].

$$\begin{cases} 1-\frac{\left|x_n^{(i)}-a(c)\right|}{\delta a}, \ (a) \\ if the\ slope\ is\ (+)\ and\ 1 \le c \le 2*N+1 \\ 1-\frac{\left|x_n^{(i)}-a(c)+\delta a\right|}{\delta a}, \ (b) \\ if\ the\ slope\ is\ (-)\ and\ 1 \le c \le 2*N+1 \end{cases} \tag{1}$$

Where:
$m$ is the degree of membership obtained.
$x_n^{(i)}$ is the input (or output) variable.
$\delta a$ is the width of the base of the triangular function.
$i$ is the fuzzy rule.
$N$ is the number of fuzzy subspaces.

### *C. Fuzzification*

The fuzzy subspace in which the variable would be entered is taken into account within a loop by which it sweeps the entire domain of the input space of the variable. It aims to obtain the position of the fuzzy subspaces which the variable enters and the degrees of membership thereof; at the end of the loop, these two values are stored in different matrices.

The maximum degree of membership is stored in a matrix and another matrix stores three vectors, the position or precise fuzzy space in which the variable for the three variables is first entered. The dimension of these matrices is 2 * N + 1 columns and the same number of rows as the column vector or column vectors where the values extracted in the previous stage are found, obtaining 730 generated rules.

Rules were repetitive, so it was necessary to use the MATLAB® function called Unique. This function detects all the values, elements, columns, rows that repeat a matrix or vector. Thus, the rows that are repeated in the matrix are captured and saved the ¨If¨ part and then performs an iterative process but this time from row to row compared to the original rule matrix with the one obtained through the Unique function, thus discarding the rows that are repeated and also have the same lower degree of membership.

Because this problem appears as a time series prediction, fuzzy subspaces are generated for both the input and the output variables. That is, there are three sets of fuzzy rules with which combines and predicts the three variables, each behaving as an output variable and using the other two remaining as input variables in each set, as shown in the block diagram of Figure 1, with which a prediction in time of the three variables treated (radiation M, ambient temperature *T*, and relative humidity H).

### *D. Defuzzification*

The defuzzification stage uses the same strategies when entering a variable in its input space. For this reason, much of the code has identical characteristics. The main difference is that a comparison is made between the position where each of the variables was entered and the previous saved position of each generated rule. Likewise, it makes a scan comparing the current row (position where the variable is entered) with each row of the matrix that contains the generated rules.

Finally, the objective to create a matrix with the pairs of data necessary to be able to satisfy equations (2) and (3) [20].

$$m_{\Delta^i}^i = m_{I_1^i}(\boldsymbol{x_1}) m_{I_2^i}(\boldsymbol{x_2}) \tag{2}$$

Where:
$\Delta^i$ Represents the output region of the rule i.
$I_j^i$ Represents the input region of rule i for component j, j is the variable or input data.

$$y = \frac{\sum_{i=1}^{K} m_{\Delta^i}^i \bar{y}^i}{\sum_{i=1}^{K} m_{\Delta^i}^i} \tag{3}$$

Where:
$\bar{y}^i$ Represents the center of the region $\Delta^i$, in this place, the degree of membership for said output region is equal to 1.

$K$ is the number of rules combined in the fuzzy rule base when the variables enter each one in their respective input spaces.

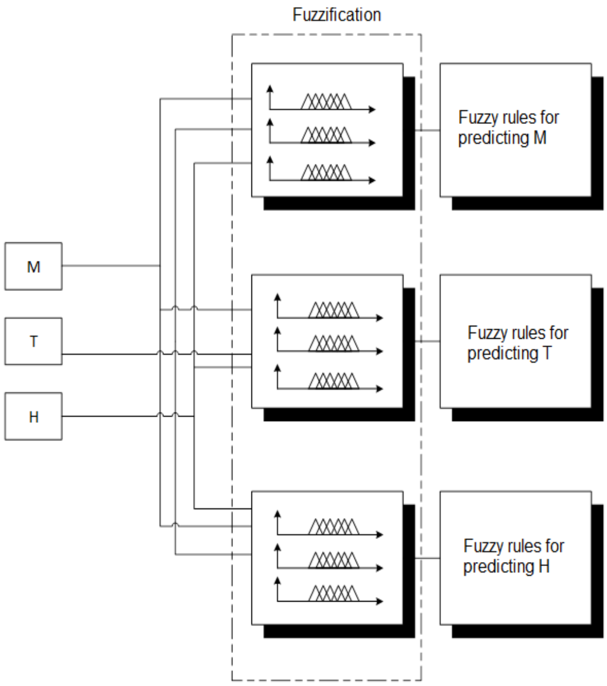


Fig. 1 Block diagram of fuzzy rule generation.

Equation (4) is a matrix with 4 pairs of elements, the first column represents all the combinations that can occur between the degrees of membership obtained at the time of entry for each variable in its respective input spaces, which is a product between degrees and in the second column is occupied by the output variable resulting from the matrix of fuzzy rules which the variable that we want to predict such as temperature, relative humidity or radiation. This represents the center of each diffuse subspace or the place corresponding to the triangle's tip within the input space.

$$\bar{\bar{Y}} = \begin{bmatrix} m_1(x_1) * m_1(x_2) & \bar{y} \\ m_2(x_1) * m_2(x_2) & \bar{y} \\ m_1(x_1) * m_2(x_2) & \bar{y} \\ m_2(x_1) * m_1(x_2) & \bar{y} \end{bmatrix} \quad (4)$$

Where:
$m_1(x_1)$ is the degree of membership for the fuzzy subspace where variable 1 enter first.
$m_2(x_1)$ is the degree of membership for the fuzzy subspace where variable 1 enters second.
$m_1(x_2)$ is the degree of membership for the fuzzy subspace where variable 2 enter first.
$m_2(x_2)$ is the degree of membership for the fuzzy subspace where variable 2 enters second.
$\bar{y}$ is the central value of the subspace of the output variable of the fuzzy rule that coincides with the input data of the corresponding input variables.

To find one of the elements involved in column 2 of (4), the procedure shown in Figure 2 is followed, which exemplifies obtaining one of the variables such as H (relative humidity).

Figure 2 shows the comparison between the input position vector of the two input variables and the matrix containing the if part's rules. Figure 2 also represents the input of each variable in its respective input subspace, and it can be seen that for each entry of a variable corresponding to two fuzzy subspaces, which finally leads to having in column 1 of (4) four possible combinations between the degrees of membership in each entry of data of the space domain with the two input variables that are involved. Once this matrix of 2 rows and 4 columns is obtained, the mathematical operation shown in (3) is calculated, which was predicted from the variable's value.

### *E. Prediction of global irradiance*

With the process carried out in the previous stage, there are three vectors with predicted values for 20 years, that is, 7300 days, but to be able to visualize and validate the prediction process correctly is necessary that the variable of interest for the particular case will be used (radiation) to contrast the information. Two curves are graphed, the first one with the already known radiation data extracted in the first stage, and in the second graph the values predicted by the network. However, these will extend to 20 years.

After obtaining the maximum global solar irradiance for each day, the following purpose is to find the global solar irradiance distribution from expression (5) [7]:

$$J(x) = M * \exp\left(-\delta * \frac{x^2}{L^2}\right) \quad (5)$$

Where:
$M$ is the amplitude of the function for the maximum radiation of the day.
$\delta$ tuning parameter.
$x$ is the time difference on periods of one hour between the moment the prediction of global solar radiation $J(x)$ is given and solar noon.
$L$ represents half the number of daylight sixths.

The number of daylight sixths because the city of Quito is located at a latitude of 0 °, the variation of hour angle is tiny throughout the year, so it remains constant between 90 and -90 degrees. Consequently, the number of daylight sixths is equal to 12 hours, corresponding to the number of hours in which the solar resource is available.

The MATLAB® function called fitlm was used allowed to find δ of (5) with the least squares' method. The δ calculated varies according to the day. However, it depends on whether there are data to obtain it, but since a prediction is being made only of the maximum global solar irradiance, the data to obtain δ would be insufficient; therefore, the script performs an average between all the δ values obtained with available data from the measurements made by the meteorological station [5]. The respective global solar irradiance distribution can finally be found for each day during all years that the prediction is calculated.

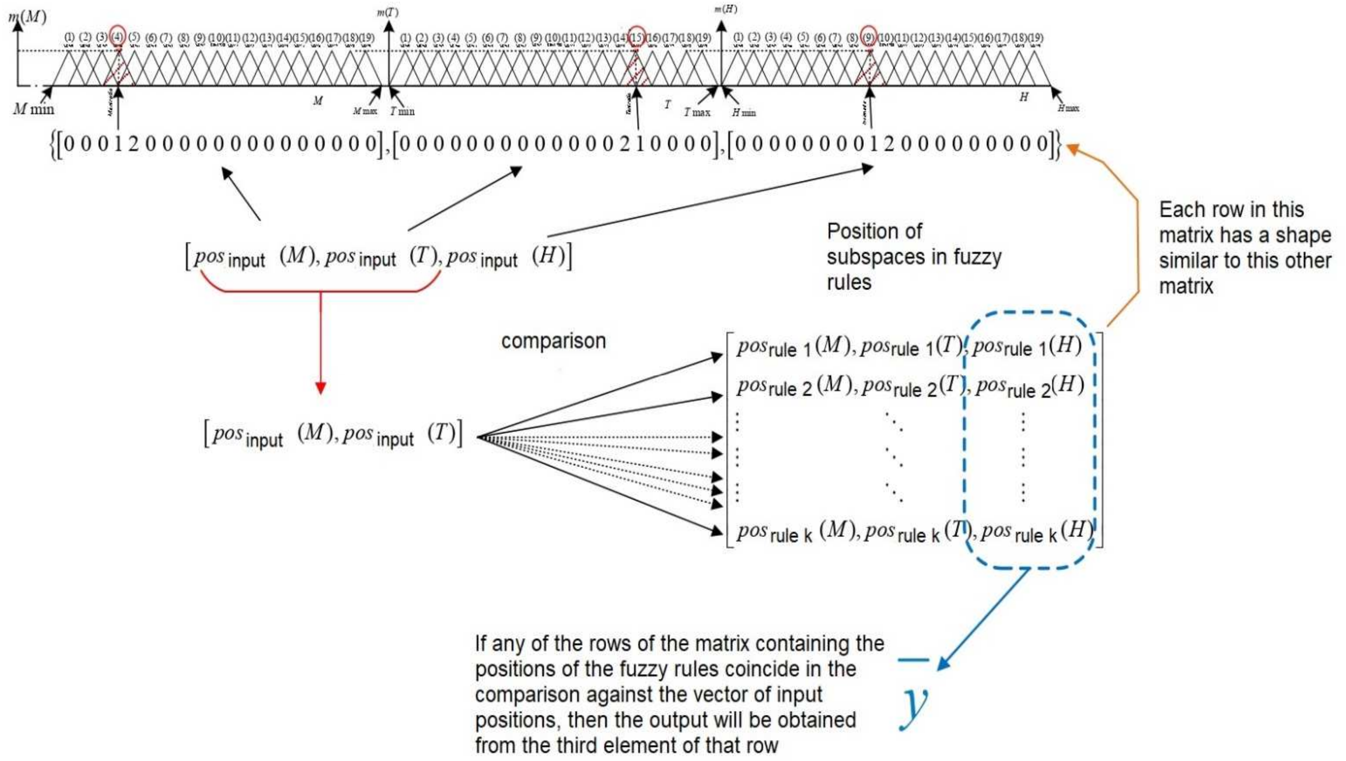


Fig. 2 Example of a section of the defuzzification of a variable.

Figure 3 shows the global solar irradiance distribution J(x) in (W/m2) for any given day and compares the real and measured distribution. It is highlighted in yellow that the maximum global solar irradiance (M) is very close to the measurement, as well the calculated and measured shape of the distribution of the global solar irradiance are similar.

### *F. Estimation of the Number of Panels*

Equations (6), (7), (8), (9), and (10) and reference [21] show the prediction calculation of the number of panels. The parameters used are shown in Table 1.

$$I_{PANEL} = N_p * I_{ph} - N_p * I_o * \Delta \tag{6}$$

Where:
$I_{PANEL}$ is the current delivered by the set of solar cells or photovoltaic panel.
$I_{ph}$ is the photogenerated current.
$N_p$ is the number of photovoltaic modules connected in parallel.
$I_o$ is a factor that represents the reverse saturation current of the diode given in (7):

$$I_o = I_{o_{ref}} * \left(\frac{T_c}{T_{ref}}\right)^3 * \exp\left(\frac{q*Eg\left(\frac{1}{T_{ref}} - \frac{1}{T_c}\right)}{K*A}\right) \tag{7}$$

Where:
$Eg$ is the energy of the semiconductor in the forbidden band, in this case for silicon it is equal to 1.11 eV at a temperature of 300 K.
$T_c$ is the working temperature of the photovoltaic panel in K that varies over time.
$A$ equals the ideality factor (0.98291 Ω)
$T_{ref}$ = 298 K
$q$ equals the charge of the electron ( $1.6 * 10^{-19}$ coulombs)
$K$ is the Boltzmann constant ( $1.38 * 10^{-23}$ J/°K = $8.61\,73\,324 * 10^{-5}$ eV/°K)
$I_{o_{ref}}$ is given in (8):

$$I_{o_{ref}} = \frac{I_{SC}}{exp\left(\frac{q*V_{OC}}{N_S*K*A*T_c}\right)} \tag{8}$$

Where:
$I_{SC}$ is the short-circuit current in A.
$V_{OC}$ is the open-circuit voltage given by the manufacturer.
$A$ is the ideality factor.
$K$ is Boltzmann's constant.
$T_c$ is the working temperature of the solar panel in K variable over time.
$q$ is the charge of the electron ( $1.6 * 10^{-19}$ coulombs).
The photogenerated current $I_{ph}$ is given in (9):

$$I_{ph} = \frac{R}{R_{ref}}\left(I_{SC} + U_{I_{SC}}\left(T_c - T_{ref}\right)\right) \tag{9}$$

Where:
$R$ is the radiation that varies in time.

| Day number: | 720 |
|---|---|
| $J(x)$ measured | $J(x)$ predicted |
| 40.1000 | 17.8202 |
| 239.0000 | 58.9265 |
| 448.4000 | 156.7734 |
| 649.7000 | 335.5815 |
| 625.8000 | 577.9466 |
| 611.6000 | 800.8322 |
| 937.3000 | 892.8108 |
| 522.6000 | 800.8322 |
| 274.6000 | 577.9466 |
| 258.9000 | 335.5815 |
| 217.7000 | 156.7734 |
| 118.9000 | 58.9265 |
| 5.4000 | 17.8202 |

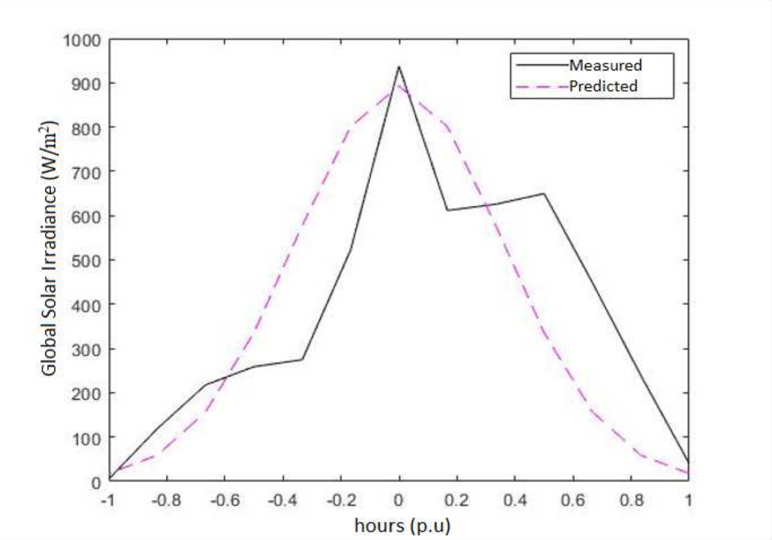


Fig. 3 Example of obtaining J (x) in one day

$R_{ref}$ is the ideal radiation for a clear sky equal to 1000 W/m$^2$.
$I_{SC}$ is equal to the short-circuit current that the manufacturer of the photovoltaic panel gives.
$T_c$ is the working temperature of the photovoltaic panel in K that varies over time.
$U_{I_{SC}}$ is the temperature coefficient for short circuit that is given by the manufacturer.

The Delta coefficient (Δ) is expressed in (10):

$$\Delta = \exp\left(\frac{q*V}{N_S*K*A*T_C}\right) - 1 \qquad (10)$$

Where:
$V$ is the nominal voltage.
$N_s$ is the number of photovoltaic panels connected in series that forms a photovoltaic module.

TABLE I
PARAMETERS USED IN ESTIMATING THE NUMBER OF PANELS.

| Parameter | Value | Units | Description |
|---|---|---|---|
| Isc | 5.34 | A | Short-circuit current |
| Tcref | 298 | K | Reference temperature |
| Ns | 14 | - | Number of cells in series to achieve the desired voltage |
| Vpanel | 18 | V | DC voltage of each cell inside the photovoltaic panel |
| Rs | 0.38707 | Ω | Series resistance of photovoltaic panel |
| Voc | 22.3 | V | Open Circuit Voltage |
| Uisc | 2.1886E-4 | %/°K | 0.060 [%/°C] |
| q | 1.6*10E-19 | eV | Electron charge |
| K | 1.38E-23 | - | Boltzmann constant |
| Tc | 308.15 | K | Typical working temperature (35°C) |
| A | 0.98291 | Ω | Ideality factor |
| Eg | 1.77842E-19 | J | Semiconductor energy in the forbidden band for Si is 1.11 eV |

The procedure to find the number of panels is similar to a numerical method process. Equation (6) calculates the current of the panel, but the Np value is needed that indicates the number of modules of cells in parallel necessary to be able to cover the current required by the load. Therefore, each module will be made up of 14 panels, and it is sought to equalize the right side with the left side of the equation with an iterative process, which will stop the moment the equalization occurs. There is a daily demand from hour to hour of energy, and an adequate number of panels for each hour is obtained, meaning for a year, there would be 8760 values with a certain number of panels. From all this range of values obtained, the largest of them is chosen because it represents the number of panels required in the worst-case scenario when it is the time between all the days of a specific year that would have the least solar radiation.

After the fixed number of cells have been found and consequently, the appropriate number of photovoltaic panels, the panel's dimensions are considered. Figure 4 shows the area in square meters of a panel.

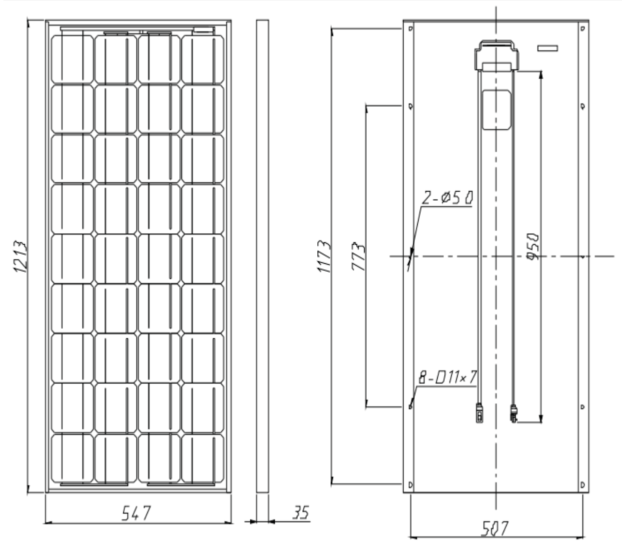


Fig. 4 Canadian Solar CS5C 90M photovoltaic panel diagram. Dimensions in mm.

Then, this area is compared with the square meters necessary to carry out the installation. If the previously obtained number of photovoltaic panels is correct, these dimensions will be used, or it will be changed if it needs to be corrected to meet the specification of the place to be installed.

## III. Results and Discussion

The load of the building of the Faculty of Civil Engineering of the Central University of Ecuador was chosen as an example, which is located in the Miraflores - Belisario sector, of the Metropolitan District of Quito, near the meteorological station from where data were collected to make the prediction of Solar Irradiance. There are the minimum and maximum power measurement data obtained from a power analyzer, which measure power data for a week every 15 minutes. Figure 5 shows the measurements made during the month of November 2019.

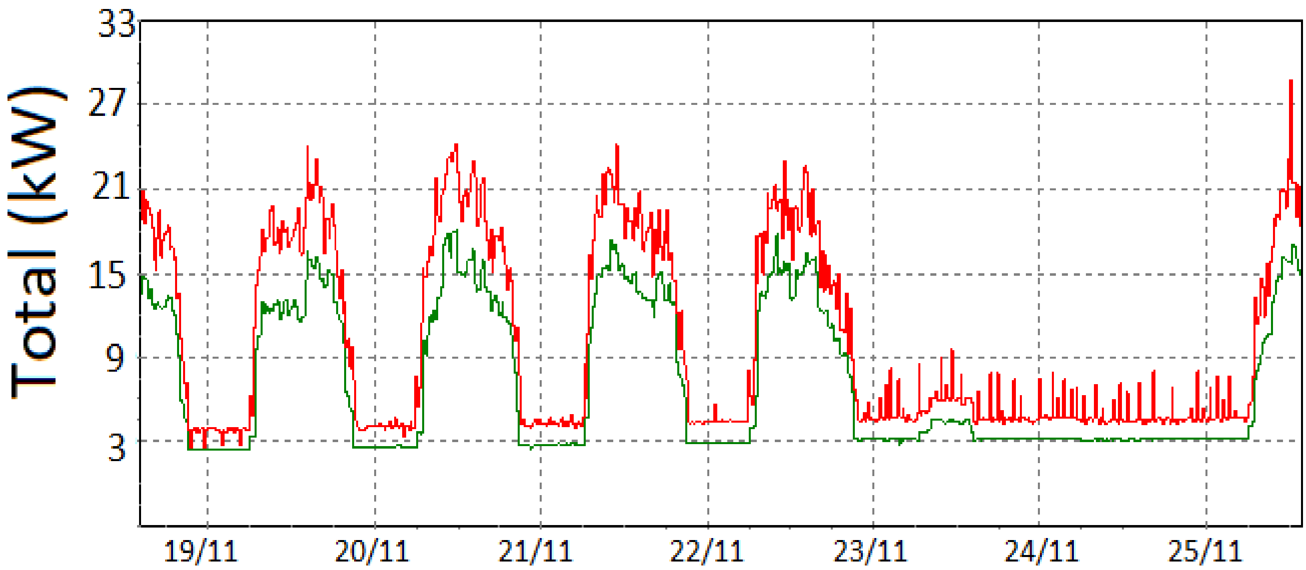


Fig. 5 Power measurements of the load corresponding to the building of the Faculty of Civil Engineering of the Central University of Ecuador.

Considering the demand for this selected load, the minimum and maximum values existing in the total data range were selected and used as limits to create a set of random numbers. This set will later be used as a static load model to interact to the photovoltaic system by simulating the interconnection between the photovoltaic system and the load.

Figure 6 shows the details of a small part of the total data obtained to generate the distribution of maximum global solar irradiance. The period chosen was a month taken from December 15th, 2019, until January 15th, 2020. For the first fifteen days, the global solar irradiance distribution data are measured by the meteorological station; On January 1st, only the global solar irradiance distribution found through the Gaussian function is available. On the other hand, the first fifteen days presented in the graph, the curves are stacked in each daily graph to be able to visually compare the predicted data and measured data, in yellow; in blue and violet, the calculation of the global solar irradiance distribution for alphas equal to 1, 2 and 3 respectively are presented. Additionally, in magenta and a broken line are the calculation of the maximum global solar irradiance for the real alpha calculated that manages to approximate the predicted data to the real data. Finally, it is verified that the process carried out for predicting the maximum global solar irradiance and its distribution throughout the day or 12 hours that there is sunlight nearby the measured global solar irradiance distribution.

When the maximum global solar irradiance distribution was obtained for all the periods of days chosen for the prediction, these data were used to find the number of photovoltaic modules required to supply the demand that the connected load requires. The first hour in the morning and the last hour in the afternoon were where the demand increased considerably, and on the contrary, there is a lower solar irradiance and was excluded to avoid oversizing the number of parallel photovoltaic modules of the photovoltaic system.

For the total hours of 80179 (of the twenty years of prediction), the highest number of photovoltaic panels are 1236 photovoltaic modules. After the necessary number of photovoltaic modules has been obtained, this number is divided by the number of panels connected in series, which is 14 in each module to reach the desired voltage, and the number of photovoltaic panels is 89.

Now the real dimensions of the selected photovoltaic panel are taken into account, and the area available to carry out the installation of the photovoltaic system. Therefore, the area obtained is taken into account through the ideal number of panels for the system. First, it could be oversized for the system occupying a large area. This study shows that the available area is slightly larger, so 91 panels can theoretically be installed compared with the 89 calculated is negligible. Table 2 reports the technical-physical data and prices from the results obtained.

After the final number of panels have been obtained according to the dimensions of the place for installation, now it is important to find the current generated by the panel or the photovoltaic system, with the global solar radiation data previously calculated in the previous stages, and it is shown in Figure 7.

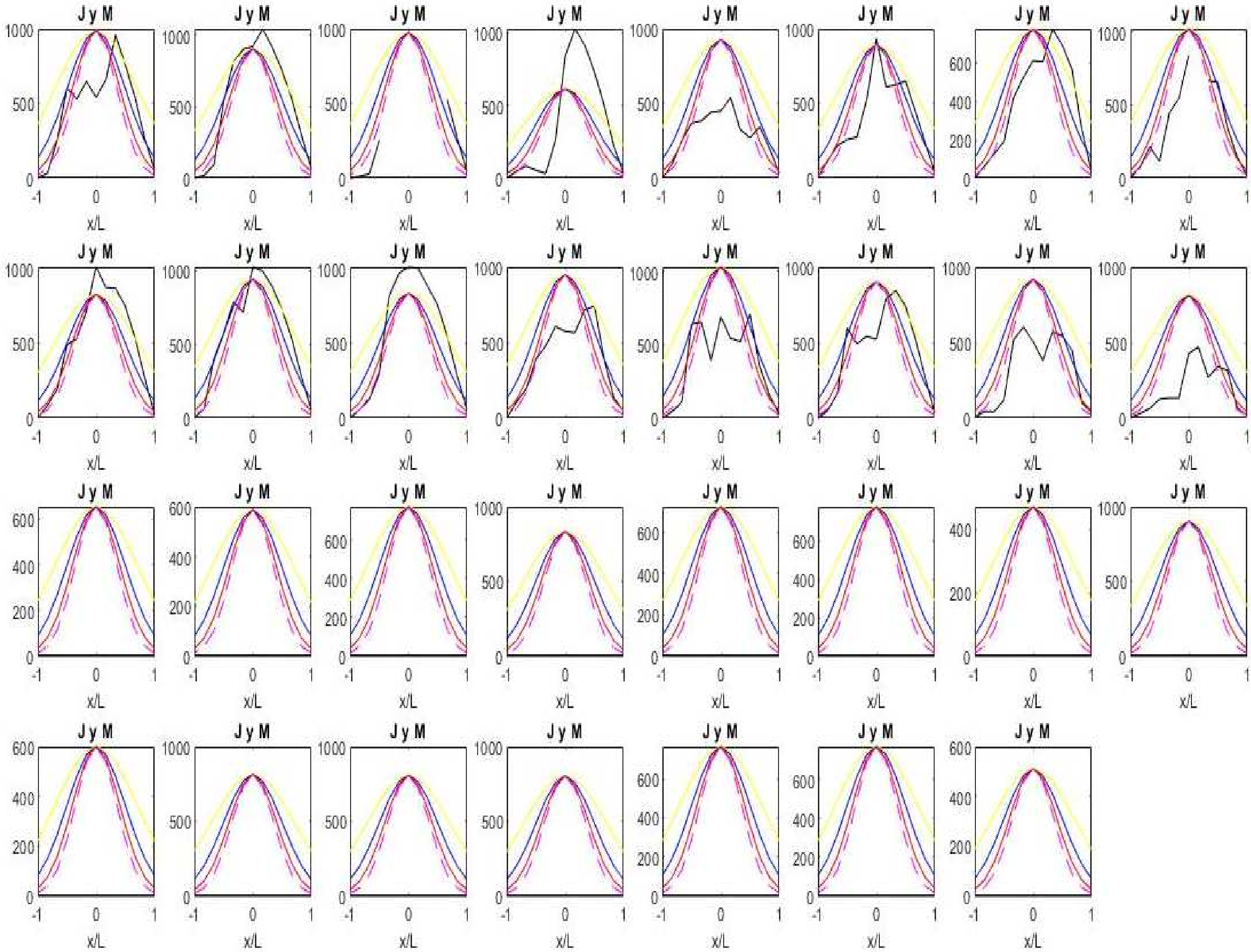


Fig. 6 Prediction of the Daily Global Solar Irradiance distribution.

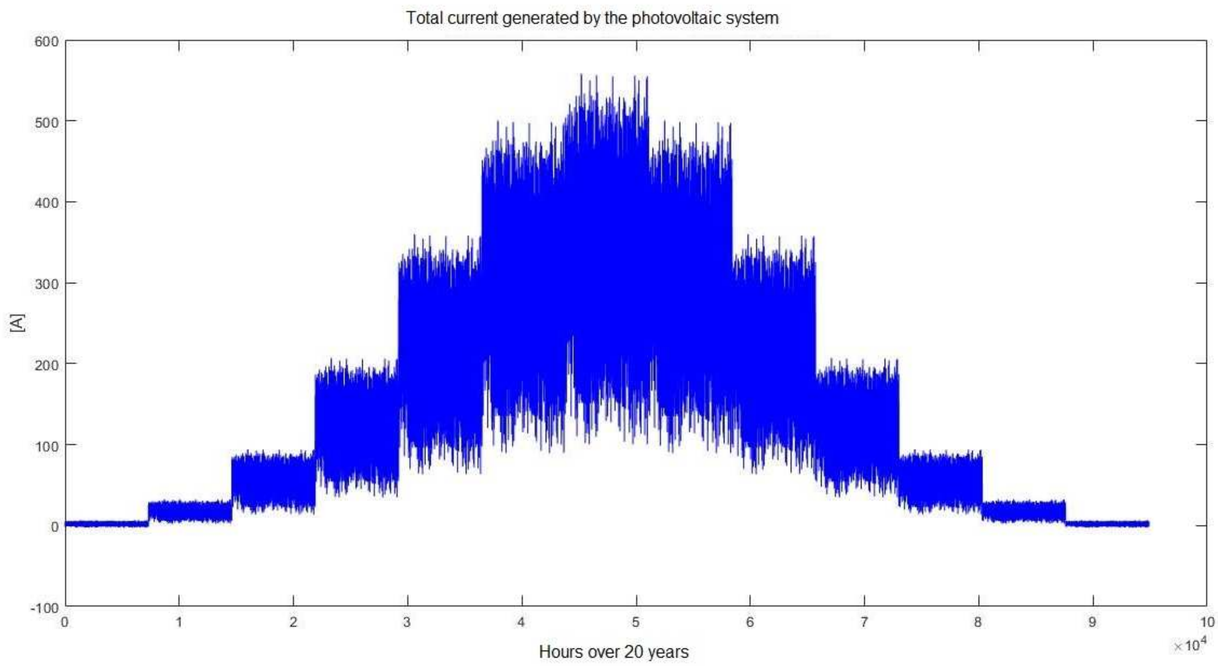


Fig. 7 The total current generated by the photovoltaic system.

With the current obtained, the product is made by the operating voltage of the installation, that is, 250 V. Figure 8 shows the power generated by the photovoltaic system with the global solar irradiance and the demand curve, for a randomly chosen day.

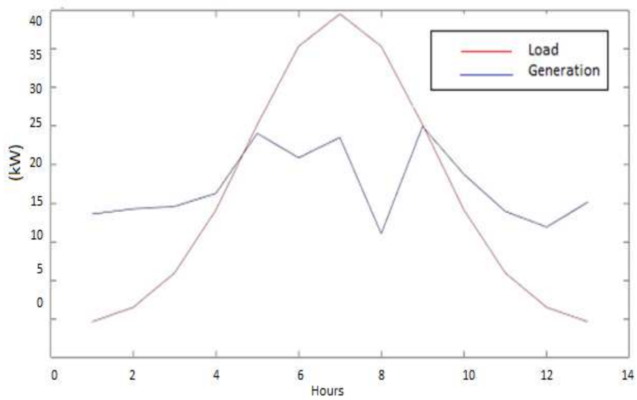


Fig. 8 Power curves generated by the photovoltaic system and load demand.

TABLE II
NUMBER OF PHOTOVOLTAIC PANELS CONSIDERING THE DIMENSIONS OF THE INSTALLATION SITE

| Parameter | Value |
|---|---|
| Number of panels calculated with the prediction | 89 |
| Number of panels calculated considering installation site dimensions | 91 |
| Panel area $m^2$ | 0,664 |
| Installation place area $m^2$ | 60 |
| Panel area without considering the installation site area $m^2$ | 0,664*89=59.09 |
| Panel area considering the installation site area $m^2$ | 0,664*91=60.42 |

Figure 9 represents the power generated by the photovoltaic system and the demand and shows the intersection section between the two curves in light blue. This area represents the demand that is satisfied through the energy delivered by the photovoltaic system. On the other hand, the remaining areas represent the excess or lack of energy that the photovoltaic system provides to the load and implies the injection or absorption of energy respectively from the distribution network where the load is also connected. It is noteworthy. Figure 9 also represents only data from one day taken randomly among the 7300 days (20 years) for which the prediction was made.

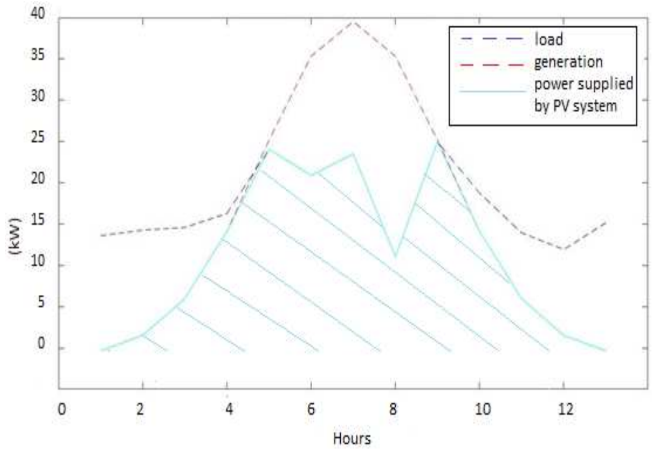


Fig. 9 Power curve that supplies the load by the photovoltaic system.

Figure 10 represents the excess or lack of energy delivered by the photovoltaic system to the load. This excess or missing energy is shown in blue and orange, respectively, for each day, during all the prediction years.

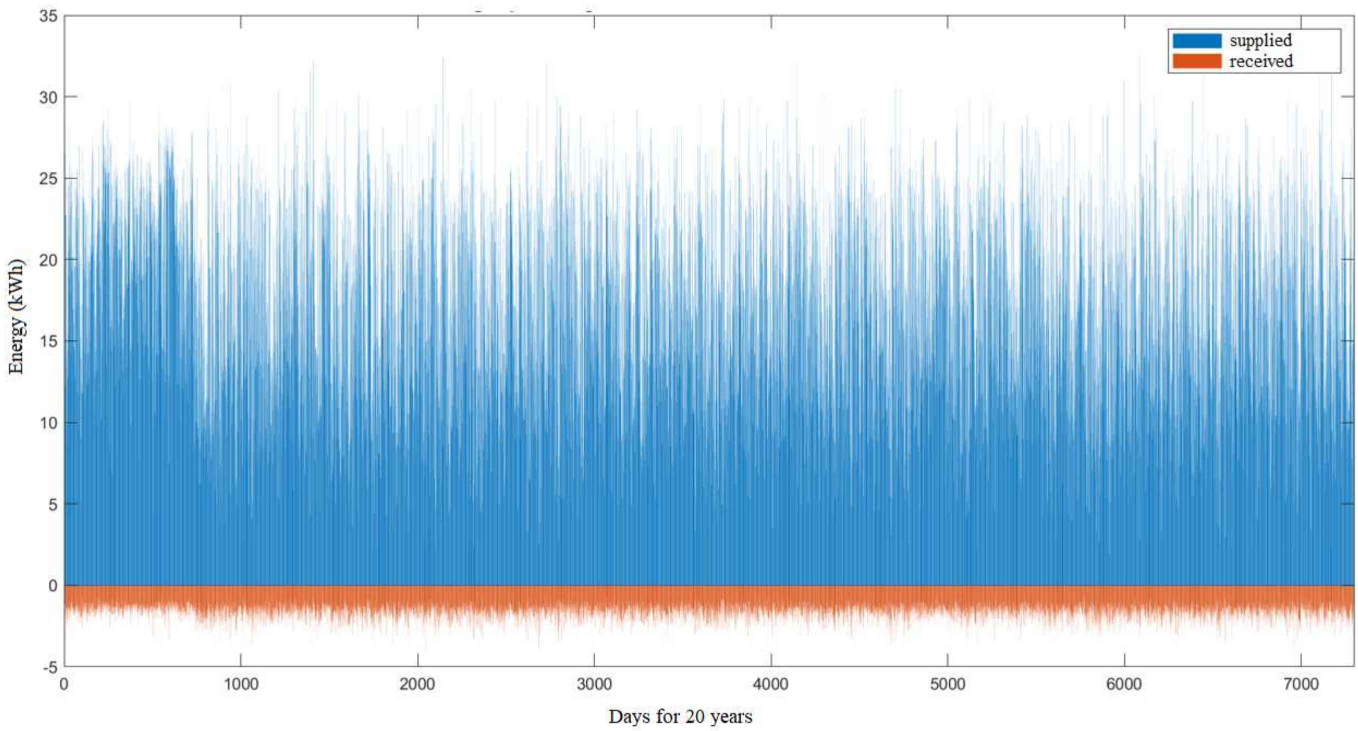


Fig. 10 Energy supplied by the photovoltaic system or received from the grid to the load.

## IV. Conclusion

For this study, solar global irradiance prediction with fuzzy logic was developed. The data of solar radiation was obtained from meteorological stations and was helpful to predict global solar irradiance with regressors. This prediction allows calculating the energy produced by a photovoltaic system over time. In addition, measuring the load demand is useful to determine the amount of excess or missing energy in a photovoltaic system connected to the grid. This quantified energy over time and through the tariff imposed by the electricity companies represents money saved or spent to power load over time, and with this, the profitability of the photovoltaic project can be calculated. Also, the prediction of energy produced compared to the load allows determining a suitable number of photovoltaic panels to avoid possible oversizing or to know the possible lack of energy capacity. The number of panels calculated also predicts the availability of space for their installation.

## References


[1] Arconel, "Generación fotovoltaica para autoabastecimiento de consumidores finales de energía eléctrica," *2018*.

[2] Arconel, "Pliego Tarifario Para Las Empresas Eléctricas De Distribución," *2020*.

[3] F. Camilo, R. Castro, M. Almeida, V. P.-S. Energy, and undefined 2017, "Economic assessment of residential PV systems with self-consumption and storage in Portugal," *Elsevier*.

[4] S. Karjalainen, H. A.-R. energy, and undefined 2019, "Pleasure is the profit-The adoption of solar PV systems by households in Finland," *Elsevier*.

[5] J. Al-Saqlawi, K. Madani, N. M. D.-E. C. and, and undefined 2018, "Techno-economic feasibility of grid-independent residential roof-top solar PV systems in Muscat, Oman," *Elsevier*.

[6] A. Duman, Ö. G.-R. Energy, and undefined 2020, "Economic analysis of grid-connected residential rooftop PV systems in Turkey," *Elsevier*.

[7] P. L. Zervas, H. Sarimveis, J. A. Palyvos, and N. C. G. Markatos, "Prediction of daily global solar irradiance on horizontal surfaces based on neural-network techniques," *Renew. Energy*, vol. 33, no. 8, pp. 1796–1803, 2008.

[8] H. Zhang, T.-W. Weng, P.-Y. Chen, C.-J. Hsieh, and L. Daniel, "Efficient Neural Network Robustness Certification with General Activation Functions," *Adv. Neural Inf. Process. Syst.*, vol. 2018-December, pp. 4939–4948, Nov. 2018.

[9] F. Ghasemi, A. Mehridehnavi, A. Pérez-Garrido, and H. Pérez-Sánchez, "Neural network and deep-learning algorithms used in QSAR studies: merits and drawbacks," *Drug Discovery Today*, vol. 23, no. 10. Elsevier Ltd, pp. 1784–1790, Oct. 2018, doi: 10.1016/j.drudis.2018.06.016.

[10] H. Wang, R. Czerminski, and A. C. Jamieson, "Neural Networks and Deep Learning," in *The Machine Age of Customer Insight*, Emerald Publishing Limited, 2021, pp. 91–101.

[11] H. Sarimveis, A. Alexandridis, G. Tsekouras, and G. Bafas, "A fast and efficient algorithm for training radial basis function neural networks based on a fuzzy partition of the input space," *Ind. Eng. Chem. Res.*, vol. 41, no. 4, pp. 751–759, 2002.

[12] E. H. C. Harik, F. Guérin, F. Guinand, J. F. Brethé, H. Pelvillain, and J. Y. Parédé, "Fuzzy logic controller for predictive vision-based target tracking with an unmanned aerial vehicle," *Adv. Robot.*, vol. 31, no. 7, pp. 368–381, Apr. 2017, doi: 10.1080/01691864.2016.1271500.

[13] A. J. Guimarães, V. J. Silva Araujo, P. V. de Campos Souza, V. S. Araujo, and T. S. Rezende, "Using fuzzy neural networks to the prediction of improvement in expert systems for treatment of immunotherapy," in *Lecture Notes in Computer Science (including subseries Lecture Notes in Artificial Intelligence and Lecture Notes in Bioinformatics)*, Nov. 2018, vol. 11238 LNAI, pp. 229–240, doi: 10.1007/978-3-030-03928-8_19.

[14] Z. Pezeshki and S. M. Mazinani, "Comparison of artificial neural networks, fuzzy logic and neuro fuzzy for predicting optimization of building thermal consumption: a survey," *Artificial Intelligence Review*, vol. 52, no. 1. Springer Netherlands, pp. 495–525, Jun. 2019, doi: 10.1007/s10462-018-9630-6.

[15] S. Jahedi Rad, M. Kaveh, V. R. Sharabiani, and E. Taghinezhad, "Fuzzy logic, artificial neural network and mathematical model for prediction of white mulberry drying kinetics," *Heat Mass Transf. und Stoffuebertragung*, vol. 54, no. 11, pp. 3361–3374, Nov. 2018, doi: 10.1007/s00231-018-2377-4.

[16] M. S. Mahmoud, *Fuzzy control, estimation and diagnosis: Single and interconnected systems*. Springer International Publishing, 2017.

[17] S. Sakunthala, R. Kiranmayi, and P. N. Mandadi, "A review on artificial intelligence techniques in electrical drives: Neural networks, fuzzy logic, and genetic algorithm," in *Proceedings of the 2017 International Conference On Smart Technology for Smart Nation, SmartTechCon 2017*, May 2018, pp. 11–16, doi: 10.1109/SmartTechCon.2017.8358335.

[18] R. Jafari, M. A. Contreras, W. Yu, and A. Gegov, "Applications of Fuzzy Logic, Artificial Neural Network and Neuro-Fuzzy in Industrial Engineering," *Mech. Mach. Sci.*, vol. 86, pp. 9–14, 2020, doi: 10.1007/978-3-030-45402-9_2.

[19] Secretaría de Ambiente de Quito, Sistema de Información Ambiental Distrital.

[20] L. X. Wang and J. M. Mendel, "Generating fuzzy rules by learning from examples," *IEEE Trans. Syst. Man. Cybern.*, vol. 22, no. 6, pp. 1414–1427, 1992.

[21] H. L. Tsai, C. S. Tu, and Y. J. Su, "Development of generalized photovoltaic model using MATLAB/SIMULINK," in *Proceedings of the world congress on Engineering and computer science*, 2008, vol. 2008, pp. 1–6.